Molecular-orbital structure in neutron-rich C isotopes

N. Itagaki,[1,*] S. Okabe,[2] K. Ikeda,[3] and I. Tanihata[3]
[1]*Department of Physics, University of Tokyo, Hongo, Tokyo 113-0033, Japan*
[2]*Center for Information and Multimedia Studies, Hokkaido University, Sapporo 060-0810, Japan*
[3]*The Institute of Physical and Chemical Research (RIKEN), Wako, Saitama 351-0198, Japan*
(Received 17 January 2001; published 30 May 2001)

The moleculelike structure of the C isotopes ($A=12$, 14, 16) is investigated using a microscopic $\alpha+\alpha+\alpha+n+n+\cdots$ model. The valence neutrons are classified based on the molecular-orbit model, and both π orbit and σ orbit are introduced around three α clusters. The valence neutrons which occupy the π orbit increase the binding energy and stabilize the linear chain of 3α against the breathinglike breakup. However, ^{14}C with the π orbit does not show a clear energy minimum against the bendinglike path. The combination of the valence neutrons in the π and σ orbits is promising to stabilize the linear-chain state against the breathing and bending modes, and it is found that the excited states of ^{16}C with the $(3/2^-_\pi)^2(1/2^-_\sigma)^2$ configuration for the four valence neutrons is one of the most promising candidates for such a structure.

DOI: 10.1103/PhysRevC.64.014301 PACS number(s): 21.10.−k, 21.60.Gx, 27.20.+n

I. INTRODUCTION

A survey of the moleculelike structure is one of the most challenging subjects in light neutron-rich nuclei. In Be isotopes, recently, decay into fragments of He isotopes (^{4}He, ^{6}He, ^{8}He) has been observed from the excited states of ^{10}Be [1] and ^{12}Be [2,3], and the presence of a two-center configuration is suggested. From the theoretical side, these states are studied by various models by which the molecular-orbital nature of the weakly bound neutrons around the two α clusters has been revealed [4–8].

As for multicluster configurations in light α nuclei beyond the two-center systems, the existence of $N\alpha$ states has been predicted around the threshold energy in the so-called Ikeda diagram [9]. For example, it has been suggested that the second 0^+ state of ^{12}C has an 3α-like molecular configuration [10]. However, according to many theoretical analyses [11], the state is not necessary to have a linear chain of 3α, but is described as a weak-coupling state with a triangular shape or the ^{8}Be$+\alpha$ configuration. Furthermore, a rotational band of ^{16}O with a very large moment of inertia has been observed around the 4α threshold energy region [12], and the 4α linear chain has been discussed [13,14]. However, the 4α chain has not been experimentally confirmed yet.

Recently, discussions of the well-developed cluster structure have been extended to the neutron-rich nuclei, and the role of valence neutrons which stabilize the linear-chain structure has been pointed out. For example, von Oertzen has extended his analyses for the molecular structure in Be isotopes [15] to C isotopes, and a linear-chain state consisting of 3α and valence neutrons around it has been speculated. Even if the 3α system without valence neutrons (^{12}C) does not have a linear-chain structure, the valence neutrons around it are expected to increase the binding energy and stabilize the linear-chain state.

In this paper, the molecular-orbital approach introduced for the Be isotopes is applied to a study of C isotopes ($A=12$, 14, 16). The appearance of prolonged structure with the α-α core in ^{10}Be [8] and ^{12}Be [16] has been successfully described by the $\alpha+\alpha+n+n+\cdots$ model, where the orbits for the valence neutrons are classified based on the molecular-orbit (MO) model [17]. In the present study, the MO is extended to C isotopes, and we focus on the stabilization of the linear-chain structure with the 3α core to which valence neutrons are added.

II. MODEL

The total wave function of a microscopic $\alpha+\alpha+\alpha+n+n\cdots$ model is fully antisymmetrized and expressed by a superposition of basis states centered on different relative distances between the α clusters (d) with various configurations of the valence neutrons ($c1, c2, \ldots$) around the α clusters:

$$\Phi^J_{MK}=\sum_{d,c1,c2\cdots} P^J_{MK}\mathcal{A}[\phi_1^{(\alpha)}\phi_2^{(\alpha)}\phi_3^{(\alpha)}(\phi_1^{c1}\chi_1)(\phi_2^{c2}\chi_2)\cdots]. \tag{1}$$

The projection to the eigenstates of angular momentum (P^J_{MK}) is performed numerically. Each α cluster consisting of four nucleons is described by Gaussians ($G_{\alpha i}$) centered at $R_{\alpha i}$ and the spin-isospin wave function (χ):

$$\phi_i^{(\alpha)}=G^{p\uparrow}_{R_{\alpha i}}G^{p\downarrow}_{R_{\alpha i}}G^{n\uparrow}_{R_{\alpha i}}G^{n\downarrow}_{R_{\alpha i}}\chi_{p\uparrow}\chi_{p\downarrow}\chi_{n\uparrow}\chi_{n\downarrow}, \quad i=1,2,3, \tag{2}$$

$$G_R=\left(\frac{2\nu}{\pi}\right)^{3/4}\exp[-\nu(\vec{r}-\vec{R})^2], \quad \nu=1/2\beta^2, \tag{3}$$

where the oscillator parameter (β) is equal to 1.46 fm. For the linear-chain state, the values of $\{R_{\alpha i}\}$ are $-d$, 0, and $+d$ on the z axis. Each valence neutron ($\phi_i^{ci}\chi_i$) around the α-α-α core is expressed by a linear combination of local Gaussians:

*Email address: itagaki@phys.s.u-tokyo.ac.jp

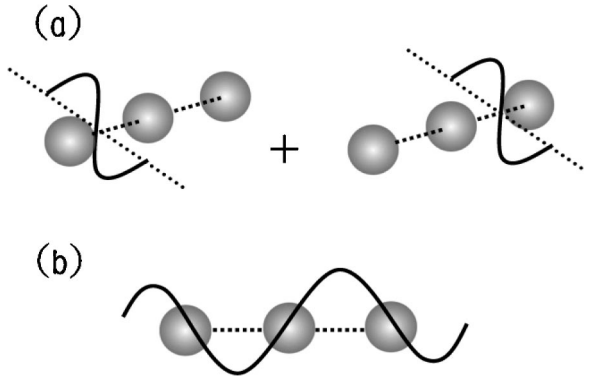

FIG. 1. The schematic figure for the amplitude of the π orbit (a) and the σ orbit (b) on the x-z plane. The circles represent the α clusters.

$$\phi_i^{ci}\chi_i = \sum_j g_j G_{R_j}\chi_i . \tag{4}$$

These valence-neutron orbits are classified according to the MO picture [17]. The orbit of the valence neutron perpendicular to the z axis of the 3α linear-chain core is called the π orbit, and the one along the z axis is called the σ orbit. Antisymmetrization imposes the forbidden space for the valence neutrons; the π orbit must have at least one node perpendicular to the z axis, and the σ orbit must have at least three nodes since three α clusters along the z axis already occupy orbitals with $n_z = 0,1,2$. The amplitudes of the π and σ orbits are schematically drawn in Fig. 1.

In the present framework, each valence-neutron orbit is introduced to have a definite K^π value at the zero limit of centers of local Gaussians ($\{R^j\}$) describing the spatial distribution of the orbit. The precise positions of $\{R^j\}$ are determined variationally before the angular momentum projection. Since the values of $\{R^j\}$ are optimized to be finite, the orbits are not exactly the eigenstate of K^π and are labeled as $\overline{K^\pi}$. For the π orbit with $\overline{K^\pi} = 3/2^-$ ($|3/2^-_\pi\rangle$), the spatial part and the spin part of $\overline{K}$ are defined to be parallel ($rY_{11}|n\uparrow\rangle$), for which the spin-orbit interaction acts attractively. At the same time, $|3/2^-_\pi\rangle$ is described as a linear combination of two orbits centered at the right- and left-hand sides of the system based on the MO picture:

$$|3/2^-_\pi\rangle = \frac{1}{\sqrt{N_\pi}}\left\{\frac{1}{\sqrt{2}}(p_x+ip_y)_{+a}+\frac{1}{\sqrt{2}}(p_x+ip_y)_{-a}\right\}|n\uparrow\rangle, \tag{5}$$

$$(p_x)_{\pm a} = G_{\pm a\vec{e}_z + b\vec{e}_x} - G_{\pm a\vec{e}_z - b\vec{e}_x},$$

$$(p_y)_{\pm a} = G_{\pm a\vec{e}_z + b\vec{e}_y} - G_{\pm a\vec{e}_z - b\vec{e}_y}. \tag{6}$$

Here, $(p_x+ip_y)_{\pm a}$ denotes the p orbit centered at $\pm a$ on the z axis, and these variational parameters a and b are optimized by using the cooling method in antisymmetrized molecular dynamics (AMD) [18,19] for each basis state. Furthermore, the $|1/2^-_\pi\rangle$ orbit where the spin-orbit interaction acts repulsively can also be defined by changing the spin direction of $|3/2^-_\pi\rangle$, where the spatial part and the spin part of $\overline{K}$ are antiparallel ($rY_{11}|n\downarrow\rangle$):

$$|1/2^-_\pi\rangle = \frac{1}{\sqrt{N_\pi}}\left\{\frac{1}{\sqrt{2}}(p_x+ip_y)_{+a}+\frac{1}{\sqrt{2}}(p_x+ip_y)_{-a}\right\}|n\downarrow\rangle. \tag{7}$$

The distribution of the σ orbit is just along the 3α axis; then, it is introduced to have three nodes. $|1/2^-_\sigma\rangle$ is represented as a linear combination of three orbits with $\overline{K^\pi} = 1/2^-$, whose centers are $+a$, 0, and $-a$ on the z axis:

$$|1/2^-_\sigma\rangle = \frac{1}{\sqrt{N_\sigma}}\{(p_z)_{+a}-(p_z)_0+(p_z)_{-a}\}|n\uparrow\rangle, \tag{8}$$

$$(p_z)_{\pm a} = G_{a\vec{e}_z + b\vec{e}_z} - G_{a\vec{e}_z - b\vec{e}_z}, \quad (p_z)_0 = G_{b\vec{e}_z} - G_{-b\vec{e}_z}. \tag{9}$$

These three orbits ($|3/2^-_\pi\rangle$, $|1/2^-_\pi\rangle$, and $|1/2^-_\sigma\rangle$) are the basic building blocks for the molecular-orbital structure. Also, $|-3/2^-_\pi\rangle$, $|-1/2^-_\pi\rangle$, and $|-1/2^-_\sigma\rangle$ orbits are introduced by taking the time reversal of $|3/2^-_\pi\rangle$, $|1/2^-_\pi\rangle$, and $|1/2^-_\sigma\rangle$ orbits, respectively.

The Hamiltonian and the effective nucleon-nucleon interaction are the same as in Refs. [8,16], and parameters of Volkov No. 2 [20] for the central part and the G3RS spin-orbit term [21] for the spin-orbit part are determined from the $\alpha+n$ and $\alpha+\alpha$ scattering phase shifts, and the binding energy of the deuteron is also reproduced with these parameters.

III. RESULTS AND DISCUSSIONS FOR BENDING STABILITY

In the following part, we show the calculated results for the stability of the linear-chain state for various configurations. The isotopes and configurations which we take into account are ^{12}C, ^{14}C$(3/2^-_\pi)^2$ (two n's in the π orbits), ^{14}C$(1/2^-_\sigma)^2$ (two n's in the σ orbits), ^{16}C$((3/2^-_\pi)^2(1/2^-_\pi)^2)$ (four n's in the π orbits), and ^{16}C$((3/2^-_\pi)^2(1/2^-_\sigma)^2)$ (two n's in the π orbits and two n's in the σ orbits). As schematically shown in Fig. 2, two variational paths are introduced corresponding to the breathinglike [Fig. 2(a)] and the bendinglike [Fig. 2(b)] degrees of freedom. The parameters d and θ stand for the α-α distance and the bending angle of the 3α core, respectively.

First, we show the 0^+ energy curves for the linear-chain structure against the breathing path in Fig. 3. It is found that the energy pocket around $d=3$ fm becomes deeper as the number of valence neutrons in the π orbit [^{12}C $\rightarrow$ ^{14}C$(3/2^-_\pi)^2 \rightarrow$ ^{16}C$((3/2^-_\pi)^2(1/2^-_\pi)^2)$]. Using our framework, the binding energy of one α cluster is calculated to be 27.5 MeV; then, the $\alpha+\alpha+\alpha$ threshold energy is -82.5 MeV, and this value is the same for the $\alpha+\alpha+\alpha+n$ neutron threshold. The 3α system (^{12}C) has minimal energy around $d=3.5$ fm; however, this is too shallow to conclude the stability of the linear-chain state. On the con-

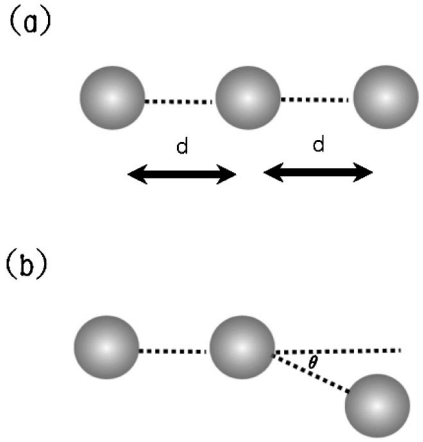

FIG. 2. The schematic figure for the breathing (a) and the bending (b) motion of the linear-chain state. The stability of the linear-chain state is examined for the α-α distance [d in (a)] and bending angle [θ in (b)].

trary, in $^{14}C(3/2^-_\pi)^2$, there appears evident minimal energy around $d=3$ fm. The energy (~ -82 MeV) is lower than ^{12}C by 11 MeV and the energy pocket is much deeper. After superposing states with different d values, this energy corresponds to the excitation energy of 18 MeV from the ground state calculated with an equilateral-triangle configuration for the 3α core, which is -101.2 MeV. The $^{16}C((3/2^-_\pi)^2(1/2^-_\pi)^2)$ configurational state is most stable among states studied and has an energy pocket of ~ -86 MeV, where the α-α distance is $d=2.5$ fm, shorter than those for ^{12}C and $^{14}C(3/2^-_\pi)^2$. Therefore, the π orbit is found to stabilize the linear-chain structure as the increase of valence neutrons

$$[^{12}C \rightarrow {}^{14}C(3/2^-_\pi)^2 \rightarrow {}^{16}C((3/2^-_\pi)^2(1/2^-_\pi)^2)].$$

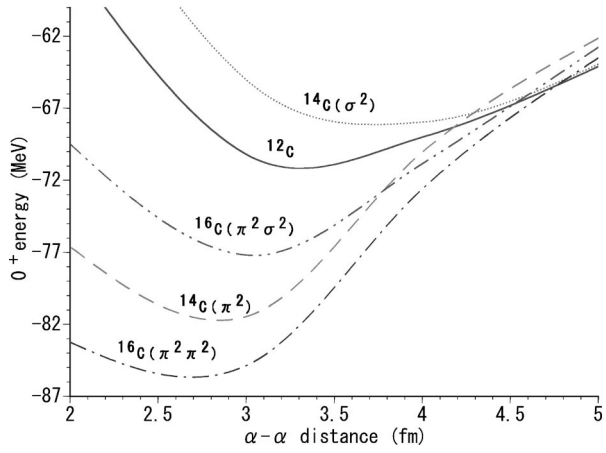

FIG. 3. The 0^+ energy curves against the α-α distance (d) for ^{12}C (solid curve), $^{14}C((3/2^-_\pi)^2)$ (dashed curve), $^{14}C((1/2^-_\sigma)^2)$ (dotted curve), $^{16}C((3/2^-_\pi)^2(1/2^-_\pi)^2)$ (dash-dotted curve), and $^{16}C((3/2^-_\pi)^2(1/2^-_\sigma)^2)$ (dashed–double-dotted curve). The 3α-threshold energy is calculated to be -82.5 MeV. The coefficients of local Gaussians $\{g_j\}$ describing the valence neutrons are treated as variational parameters to take into account deviations of the original MO.

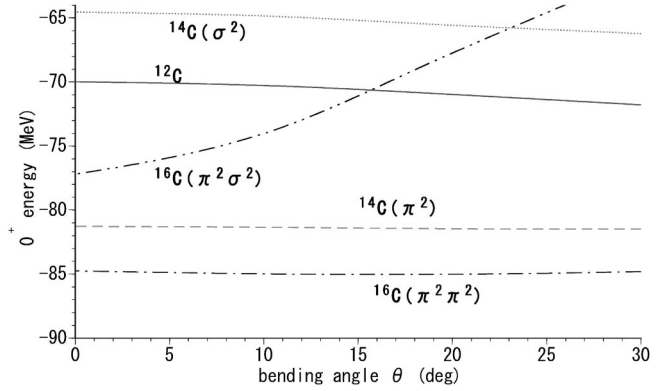

FIG. 4. The 0^+ energy curves against the bending angle (θ) for ^{12}C (solid curve), $^{14}C((3/2^-_\pi)^2)$ (dashed curve), $^{14}C((3/2^-_\sigma)^2)$ (dotted curve), $^{16}C((3/2^-_\pi)^2(1/2^-_\pi)^2)$ (dash-dotted curve), and $^{16}C((3/2^-_\pi)^2(1/2^-_\sigma)^2)$ (dashed–double-dotted curve). The 3α-threshold energy is calculated to be -82.5 MeV. The coefficients for the linear combination of Gaussians describing the MO are optimized at $\theta=0°$ and fixed. The α-α distance (d) is fixed to 3 fm.

The ground state energy of ^{16}C in this model can be estimated to be -106.7 MeV by considering the calculated ground state energy of ^{14}C and the experimental $2n$ separation energy of ^{16}C ($-101.2-5.5=-106.7$ MeV); then, this state corresponds to the excitation energy of 20 MeV region.

Next, we discuss the case where the valence neutrons occupy the σ orbit. $^{14}C(1/2^-_\sigma)^2$ has an excitation energy higher by about 14 MeV in comparison with $^{14}C(3/2^-_\pi)^2$. It is rather surprising that the difference is only 14 MeV in spite of the fact that $3/2^-_\pi$ has only one node and $1/2^-_\sigma$ has three nodes. This is because the σ orbit is along the α-α-α core: The higher nodal orbits along the symmetry axis become low lying as a result of the clustering of the core. The σ orbit enhances the prolonged shape of the 3α core, and the optimal d value is ~ 3.5 fm. However, the $^{14}C(1/2^-_\sigma)^2$ case has no deep pockets enough to be stabilized against the breathinglike path. When two more valence neutrons occupy the π orbit, although this minimal energy is higher by 5 MeV than that of $^{16}C((3/2^-_\pi)^2(1/2^-_\pi)^2)$, $^{16}C((3/2^-_\pi)^2(1/2^-_\sigma)^2)$ has a minimal 0^+ energy of ~ -77 MeV. The calculated energy pocket is deep enough to guarantee the stability for the breathinglike path. Therefore, it is summarized that the linear-chain structure cannot be stabilized against the breathinglike mode with the σ orbit only in $^{14}C((1/2^-_\sigma)^2)$; however, the neutrons in π orbits increase the binding energy and prevent the breakup of the system in

$$^{14}C((3/2^-_\pi)^2),\ ^{16}C((3/2^-_\pi)^2(1/2^-_\pi)^2),$$

and

$$^{16}C((3/2^-_\pi)^2(1/2^-_\sigma)^2).$$

Finally, the stability of these linear-chain states against the bendinglike path is examined. The 0^+ energy curves of ^{12}C, $^{14}C((3/2^-_\pi)^2)$, $^{14}C((1/2^-_\sigma)^2)$, $^{16}C((3/2^-_\pi)^2(1/2^-_\pi)^2)$, and $^{16}C((3/2^-_\pi)^2(1/2^-_\sigma)^2)$ against the θ value are shown in Fig. 4.

TABLE I. The squared overlap between $\theta=0°$ and $\theta=30°$ for ^{12}C, ^{14}C$((3/2^-_\pi)^2)$, ^{14}C$((3/2^-_\sigma)^2)$, ^{16}C$((3/2^-_\pi)^2(1/2^-_\pi)^2)$, and ^{16}C$((3/2^-_\pi)^2(1/2^-_\sigma)^2)$.

Configuration	Squared overlap between $\theta=0°$ and $\theta=30°$
^{12}C	0.906
^{14}C$((3/2^-_\pi)^2)$	0.905
^{14}C$((3/2^-_\sigma)^2)$	0.804
^{16}C$((3/2^-_\pi)^2(1/2^-_\pi)^2)$	0.865
^{16}C$((3/2^-_\pi)^2(1/2^-_\sigma)^2)$	0.602

Except for the case of ^{16}C$((3/2^-_\pi)^2(1/2^-_\sigma)^2)$, the curvature of these states is rather monotonic and the energy minimum does not clearly appear. In ^{14}C, the orthogonality between the linear-chain configuration and low-lying states with an equilateral-triangle configuration of 3α is taken into account. This effect works but not sufficiently to push up the energy of the state with a finite bending angle. However, as clearly seen in Fig. 4, the ^{16}C$((3/2^-_\pi)^2(1/2^-_\sigma)^2)$ case shows a sharp increase of the 0^+ energy as the increase of the bending angle and is found to be stable against the bendinglike path. This feature is much different from ^{12}C, ^{14}C$((3/2^-_\pi)^2)$, ^{14}C$((1/2^-_\sigma)^2)$, and ^{16}C$((3/2^-_\pi)^2(1/2^-_\pi)^2)$ cases. From the analysis above, the linear-chain configuration can be stabilized against the breathinglike path by neutrons in the π orbit [^{14}C$((3/2^-_\pi)^2)$, ^{16}C$((3/2^-_\pi)^2(1/2^-_\pi)^2)$, ^{16}C$((3/2^-_\pi)^2(1/2^-_\sigma)^2)$], but ^{16}C$((3/2^-_\pi)^2(1/2^-_\sigma)^2)$ is only the case which is stable also against the bendinglike path.

We further discuss the reason for the sharp increase of the 0^+ energy in ^{16}C$((3/2^-_\pi)^2(1/2^-_\sigma)^2)$ against the bendinglike path. The 0^+ energy increases by 15.7 MeV from $\theta=0°$ to $\theta=30°$, in which the kinetic energy part is 10.3 MeV. To understand the energy increase with the increase of the bending angle θ of this case, we calculate and compare the overlap between the wave functions with $\theta=0°$ and $\theta=30°$ for various configurations in Table I, where the results are shown. In ^{12}C, the wave functions with $\theta=0°$ and $\theta=30°$ have a squared overlap of 0.91, and ^{14}C$((3/2^-_\pi)^2)$ has almost the same value. ^{14}C$((3/2^-_\sigma)^2)$ has a value of 0.85, smaller than ^{14}C$((3/2^-_\pi)^2)$ by only 6%, and ^{16}C$((3/2^-_\pi)^2(1/2^-_\pi)^2)$ has almost the same value as the ^{14}C$((1/2^-_\sigma)^2)$ case. This result shows that the overlaps additionally decreases a little for the σ-orbital neutrons and, also, for the π-orbital neutrons as the increase of valence neutrons. In spite of these, the overlap between $\theta=0°$ and $\theta=30°$ for the ^{16}C$((3/2^-_\pi)^2(1/2^-_\sigma)^2)$ case shows a significantly large decrease to 0.60. Here ^{16}C$((3/2^-_\pi)^2(1/2^-_\sigma)^2)$ is the only configuration which shows a drastic decrease of the overlap between $\theta=0°$ and $\theta=30°$.

As discussed in the following part, it can be shown that the drastic decrease as the bending angle increases is due to the increase of the overlap between two neutrons in the π orbit and two neutrons in the σ orbit. When there arises an overlap between them, the overlap component in the total wave function is diminished due to the Pauli exclusion principle, that is, so-called Pauli blocking. Therefore, the physical state can be expressed by the modified wave function which is made by subtracting the overlap component from the original wave function. Since the energies of the π and σ orbits discussed here are relatively low, the modified wave function involves larger components of higher excitation energy in comparison with the wave function at $\theta=0$ free from Pauli blocking. As a result, Pauli blocking due to an increase of overlap between valence four neutrons is considered to bring an increase of energy proportional to the decrease of the squared overlap. This is a possible explanation for the rapid increase of the energy against the bending angle. In this view we can estimate the increase of energy as follows. First, we compare the cases with Pauli blocking and without Pauli blocking. If there is no Pauli blocking, the squared overlap of ^{16}C$((3/2^-_\pi)^2(1/2^-_\sigma)^2)$ between $\theta=0°$ and $\theta=30°$ is estimated as follows:

$$P(^{16}\mathrm{C}_{\pi\sigma})_{no\ Pauli}=\frac{P(^{14}\mathrm{C}_\pi)\times P(^{14}\mathrm{C}_\sigma)}{P(^{12}\mathrm{C})}=0.85. \quad (10)$$

Here, $P(^{14}\mathrm{C}_\pi)$, $P(^{14}\mathrm{C}_\sigma)$, and $P(^{12}\mathrm{C})$ are squared overlaps between $\theta=0°$ and $\theta=30°$ of ^{14}C$((3/2^-_\pi)^2)$, ^{14}C$((1/2^-_\sigma)^2)$, and ^{12}C shown in Table I. In the actual squared overlap of ^{16}C$((3/2^-_\pi)^2(1/2^-_\sigma)^2)$ shown in Table I, the Pauli blocking effect is automatically included, and the value is $P(^{16}\mathrm{C}_{\pi\sigma})_{with\ Pauli}=0.60$. This difference corresponds to the component excited to higher shells because of the Pauli blocking effect, and this is 25%:

$$P(^{16}\mathrm{C}_{\pi\sigma})_{no\ Pauli}-P(^{16}\mathrm{C}_{\pi\sigma})_{with\ Pauli}=0.25. \quad (11)$$

Second, we estimate the increase of kinetic energy when two valence neutrons in the π or σ orbits are excited to higher shells by 25% due to the Pauli blocking effect:

$$\Delta E=2\times\hbar\omega\times 0.25=\sim 10\ \mathrm{MeV}. \quad (12)$$

This value is consistent with the increase of the kinetic energy at $\theta=30°$ mentioned above. Therefore, we can conclude that this is one of the most important mechanisms which stabilizes the linear-chain state in ^{16}C.

IV. SUMMARY AND DISCUSSIONS

It is summarized that the linear-chain structure of ^{16}C$((3/2^-_\pi)^2(1/2^-_\sigma)^2)$ with 3α core is the only case to have simultaneous stabilities for the breathinglike breakup path and for the bendinglike path among ^{12}C, ^{14}C, and ^{16}C. Other configurations, such as ^{14}C$((3/2^-_\pi)^2)$ and ^{16}C$((3/2^-_\pi)^2(1/2^-_\pi)^2)$, are stable against the breathinglike path but not stable against the bendinglike path. A combination of the π and σ orbits occupied by four neutrons plays doubly important roles to make a deep energy pocket for the breathinglike path and to prevent the bendinglike free motion of the system. The ^{16}C$((3/2^-_\pi)^2(1/2^-_\sigma)^2)$ configuration forms a rotational band with an energy slope of $\hbar^2/2I=150$ keV. The minimal energy (~ -77 MeV) corresponds to 29 MeV in excitation, since the ground state energy of ^{16}C in this model is estimated to be -106.7 MeV. However, after per-

forming a superposition of states with different α-α distances, it is expected that the energy gain is a few MeV, and the bandhead energy corresponds to the 25 MeV region.

We have shown in ^{16}C that the Pauli-blocking effect among valence neutrons play an important role for the stability of the linear-chain configuration. This effect is expected to be more important as the neutron number increases. We are interested in the appearance in ^{18}C of a similar linear-chain structure in the low-lying region, where all of three neutron orbits introduced here are occupied $[(3/2^-_\pi)^2(1/2^-_\pi)^2(1/2^-_\sigma)^2]$.

Experimentally, the observation of γ rays from high-spin states is the most probable way to confirm the presence of a rotational band with a large moment of inertia. Although the present analysis has been restricted to the 0^+ state, we will investigate also high-spin states, where it is expected that the gluelike role of valence neutrons becomes more important to prevent the breathinglike breakup of the system.

In the present analysis, the parameter d has been fixed when the stability against the bending motion has been examined, and θ has been fixed to zero when the bending motion has been examined. However, to assure theoretically the stability of these linear-chain states, we intend to investigate the case when two degrees of freedom (d and θ) are simultaneously activated. This shall be examined by superposing states on the energy surface of d and θ based on the generator coordinate method.

ACKNOWLEDGMENTS

The authors thank members of the RI beam science laboratory in RIKEN for discussions and encouragement. One of the authors (N.I.) thanks Prof. R. Lovas, Prof. W. von Oertzen, Prof. H. Horiuchi, and Dr. Y. Kanada-En'yo for fruitful discussions.

[1] N. Soić *et al.*, Europhys. Lett. **34**, 7 (1996).
[2] A. A. Korscheninnikov *et al.*, Phys. Lett. B **343**, 53 (1995).
[3] M. Freer *et al.*, Phys. Rev. Lett. **82**, 1383 (1999).
[4] H. Furutani, H. Kanada, T. Kaneko, S. Nagata, H. Nishioka, S. Okabe, S. Saito, T. Sakuda, and M. Seya, Prog. Theor. Phys. Suppl. **68**, 193 (1980).
[5] M. Seya, M. Kohno, and S. Nagata, Prog. Theor. Phys. **65**, 204 (1981).
[6] Y. Kanada-En'yo, H. Horiuchi, and A. Doté, Phys. Rev. C **60**, 064304 (1999).
[7] Y. Ogawa, K. Arai, Y. Suzuki, and K. Varga, Nucl. Phys. **A673**, 122 (2000).
[8] N. Itagaki and S. Okabe, Phys. Rev. C **61**, 044306 (2000).
[9] K. Ikeda, N. Takigawa, and H. Horiuchi, Prog. Theor. Phys. Suppl. **Extra Number**, 464 (1968).
[10] H. Morinaga, Phys. Rev. **101**, 254 (1956); Phys. Lett. **21**, 78 (1966).
[11] Y. Fujiwara, H. Horiuchi, K. Ikeda, M. Kamimura, K. Katō, Y. Suzuki, and E. Uegaki, Prog. Theor. Phys. Suppl. **68**, 60 (1980).
[12] P. Chevallier, F. Scheibling, G. Goldring, I. Plesser, and M. W. Sachs, Phys. Rev. **160**, 827 (1967).
[13] H. Horiuchi, K. Ikeda, and Y. Suzuki, Prog. Theor. Phys. Suppl. **52**, 89 (1972).
[14] W. D. M. Rae, A. C. Merchant, and B. Buck, Phys. Rev. Lett. **69**, 3709 (1992).
[15] W. von Oertzen, Z. Phys. A **354**, 37 (1996); **357**, 355 (1997).
[16] N. Itagaki, S. Okabe, and I. Ikeda, Phys. Rev. C **62**, 034301 (2000).
[17] Y. Abe, J. Hiura, and H. Tanaka, Prog. Theor. Phys. **49**, 800 (1973).
[18] Y. Kanda-En'yo, H. Horiuchi, and A. Ono, Phys. Rev. C **52**, 628 (1995).
[19] A. Ono, H. Horiuchi, T. Maruyama, and A. Ohnishi, Prog. Theor. Phys. **87**, 1185 (1992); Phys. Rev. Lett. **68**, 2898 (1992).
[20] A. B. Volkov, Nucl. Phys. **74**, 33 (1965).
[21] N. Yamaguchi, T. Kasahara, S. Nagata, and Y. Akaishi, Prog. Theor. Phys. **62**, 1018 (1979).